Miniaturized Full-Metal Dual-Band Filter Using Dual-Mode Circular Spiral Resonators

Rui-Sen Chen, *Graduate Student Member, IEEE*, Lei Zhu, *Fellow, IEEE*, Jing-Yu Lin, *Graduate Student Member, IEEE*, Sai-Wai Wong, *Senior Member, IEEE*, Yin Li, *Member, IEEE*, Yang Yang, *Senior Member, IEEE*, and Yejun He, *Senior Member, IEEE*

***Abstract*— A miniaturized full-metal dual-band bandpass filter using a dual-mode circular spiral resonator (CSR) in a single metal cavity is proposed. Two spirals are combined together to form a dual-mode resonator, and the transmission zero (TZ) produced by the source–load coupling can separate the two modes and achieve the desired dual-band property. Then, a second-order dual-band filter is designed based on the dual-mode resonator, and each band can be individually synthesized, designed, and tuned to achieve the desired filtering performances. In addition, each band has TZs on both sides of the passband to achieve high selectivity. The size of the second-order dual-band filter is only $0.073\lambda_0 \times 0.055\lambda_0 \times 0.015\lambda_0$ calculated at the center frequency of the lower band. Finally, the filter is fabricated and measured, and a good agreement is achieved between the measurement and simulation.**

***Index Terms*— Circular spiral resonator (CSR), dual-band, dual-mode, full metal, miniaturized size, transmission zeroes (TZs).**

I. Introduction

MULTIBAND microwave devices are widely applied to the modern wireless communication systems due to the continuous development of multiple wireless standards and applications. As an essential component, multiband filters with high performance, such as low loss, compact size, and large power capacity, are highly demanded in the transceiver systems. Multiband filters have been reported in many literature works with different design methods and configurations. The multiband filters implemented on planar structures, such as the microstrip [1]–[4], the coplanar waveguide [5], and the slot line [6], have a compact size. The multiband filters designed using cavity structures, such as the rectangular and circular waveguides [7]–[10], the coaxial cavity [11]–[14], and the conductive-postloaded cavity [15], can reduce the power loss and enhance power handling. However, most of the reported full-metal multiband filters suffer from a large circuit size [16]. A filter designed using a helical resonator has a much smaller circuit compared to the aforementioned cavity filters [17]. In [18], a novel compact-size dual-band filter using a helical resonator is presented; however, it has a complicated fabrication due to its 3-D structure. In addition, except for the works in [12], [13], and [15], the aforementioned multiband cavity filters cannot achieve the individual adjustment of the external Q-factors, coupling coefficients, and frequencies.

In this letter, a miniaturized dual-band filter using a dual-mode circular spiral resonator (CSR) in a single metal cavity is proposed. The proposed dual-mode resonator is composed of two metal spirals sharing one common supporting metal strip to enhance physical support and reduce circuit size. The produced transmission zeroes (TZs) separate the two modes and achieve the dual-band property. Then, the dual-mode resonator is used to design a second-order dual-band filter. These two bands can be individually synthesized and realized to achieve different filtering performances. In addition, the proposed filter can achieve high selectivity by the TZs produced by the source–load coupling without additional structure. Finally, the proposed second-order dual-band filter is fabricated and measured with a good performance.

II. Dual-Mode CSR

To obtain a dual-mode resonator, two spirals with different sizes are placed together in the rotational symmetrical position, as shown in Fig. 1(a). The spirals' size is expressed as r_i (inner radius), g_i (gap between turns), w_i (turns' width), h_i (spirals' thickness), and n_i (number of turns), where $i = 1, 2$, corresponding to Spiral I and II. The proposed arrangement of the two CSRs has a compact size, since these two spirals share a short-circuit strip, and can also enhance the strength of the physical support of the CSRs on the walls, since it has three physical supporting points (which include the connection of the spirals and the probes). The two probes are physically close so that source–load coupling can be achieved, which can produce extra TZs [19]. The simulated S-parameter of the two-section spiral resonator is shown in Fig. 1(b). The resonant frequencies are 205 and 240 MHz, which correspond to the total length of 439.5 and 375 mm (both about $0.3\lambda_0$), respectively. The TZs are produced to separate the two modes to achieve the dual-band property.

Manuscript received March 16, 2020; revised April 16, 2020; accepted April 19, 2020. Date of publication May 7, 2020; date of current version June 5, 2020. This work was supported in part by the Shenzhen Science and Technology Programs under Grant JCYJ20180305124543176 and Grant JCYJ 20190728151457763, in part by the Natural Science Foundation of Guangdong Province under Grant 2018A030313481, in part by the Shenzhen University Research Startup Project of New Staff under Grant 20188082, and in part by the National Natural Science Foundation of China under Grant 81771955. *(Corresponding author: Sai-Wai Wong.)*

Rui-Sen Chen is with the College of Electronics and Information Engineering, Shenzhen University, Shenzhen 518060, China, and also with the Department of Electrical and Computer Engineering, Faculty of Science and Technology, University of Macau, Macau 999078, China.

Lei Zhu is with the Department of Electrical and Computer Engineering, Faculty of Science and Technology, University of Macau, Macau 999078, China.

Jing-Yu Lin and Yang Yang are with the School of Electrical and Data Engineering, University of Technology Sydney, Ultimo, NSW 2007, Australia.

Sai-Wai Wong, Yin Li, and Yejun He are with the College of Electronics and Information Engineering, Shenzhen University, Shenzhen 518060, China (e-mail: wongsaiwai@ieee.org).

Color versions of one or more of the figures in this letter are available online at http://ieeexplore.ieee.org.

Digital Object Identifier 10.1109/LMWC.2020.2990068

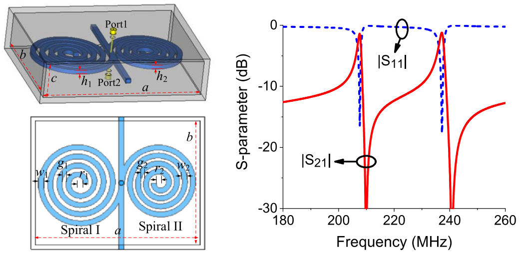

(a) (b)

Fig. 1. Proposed dual-mode spiral resonator. (a) Configuration. (b) Simulated result with $a = 113$, $b = 84$, $c = 23$, $r_1 = 2.5$, $g_1 = 2.75$, $w_1 = 3.5$, $h_1 = 3$, $n_1 = 4$, $r_2 = 2$, $g_2 = 2$, $w_2 = 3.5$, $h_2 = 3$, $n_2 = 4$. (Unit: mm, except for n_1 and n_2.)

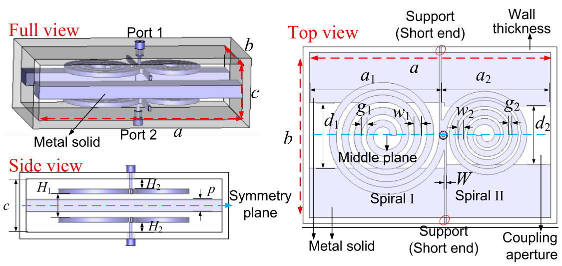

(a) (b)

Fig. 2. Proposed dual-band filter. (a) Full view and side view. (b) Top view.

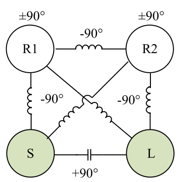

	Lower stopband	Upper stopband
S → L	+90°	+90°
S → R1 → R2 → L	(-90°) + (+90°) + (-90°) + (+90°) + (-90°) = -90°	(-90°) + (-90°) + (-90°) + (-90°) + (-90°) = -450°
Phase difference	180°	180°
TZ	Yes	Yes

(a) (b)

Fig. 3. Mechanism of the TZ of the second-order single-band filter. (a) Coupling mechanism. (b) Phase analysis of the multiple transmission paths.

The simulated unloaded Q-factors of the two resonances are about 1500, while the helical resonator reported in [17] and [18] has an unloaded Q-factor of 1250.

III. Filter Design

Based on the dual-mode resonator, a second-order dual-band filter is proposed, as shown in Fig. 2 with marked dimensions. According to the configuration of the proposed dual-band filter shown in Fig. 2, each band can be seen as a second-order single-band bandpass filter and can be individually synthesized and designed.

The coupling mechanism of the second-order single-band filter is shown in Fig. 3(a). The inductive and capacitive elements represent the magnetic and electric couplings, respectively. S, L, $R1$, and $R2$ represent the source, load, resonator 1, and resonator 2, respectively. The inductive coupling has a $-90°$ phase and the capacitive coupling has a $+90°$ phase. The resonator has a $+90°$ phase at a lower stopband and a $-90°$ phase at an upper stopband. However, the phase analysis of the multiple paths, i.e., S–L and S–$R1$–$R2$–L, is shown in Fig. 3(b). It can be seen that at both the lower and upper stopbands, the two paths are out of the phase. Thus, the signal transmitting from source to load is cancelled at certain frequencies of the lower and upper stopbands, which then produces the TZs. The coupling paths S–$R1$–L and S–$R2$–L produced by couplings M_{L1} and M_{S2} do not affect the number

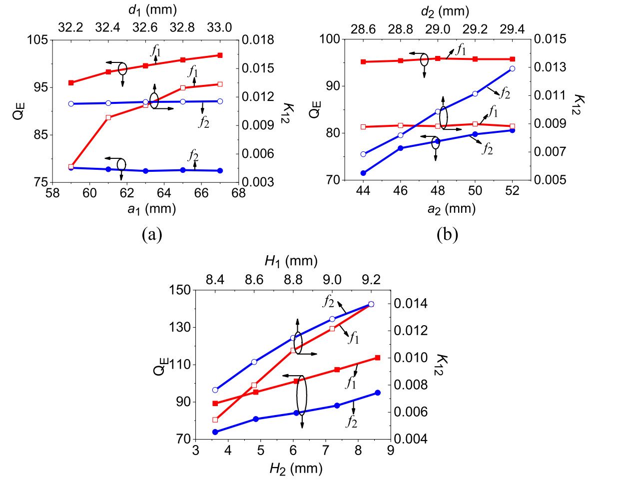

(a) (b) (c)

Fig. 4. Extraction of Q_E and K_{12}. (a) Individual adjustment of Filter-I. (b) Individual adjustment of Filter-II. (c) Simultaneous adjustments of the two filters.

of the TZs, and these two unwanted couplings cause an asymmetric position of the TZs, as discussed in [20, Sec. IV-A].

The designed targets of the dual-band filter are: 1) Band-I (Filter-I): $f_1 = 195$ MHz, FBW $= 1.5\%$, RL $= 20$ dB, $\mathrm{TZ}_1 = 160$ MHz, and $\mathrm{TZ}_2 = 200$ MHz; and 2) Band-II (Filter-II): $f_2 = 265$ MHz, FBW $= 2\%$, RL $= 20$ dB, $\mathrm{TZ}_1 = 250$ MHz, and $\mathrm{TZ}_2 = 285$ MHz. Where f_1 and f_2 are the center frequencies of the first filter and the second filter, respectively, FBW is the fractional bandwidth, RL is the return loss, and TZ is the transmission zero.

According to the specification of 1) and 2), we obtained the coupling matrixes M_1 and M_2 of these two filters [21], [22]

$$M_1 = \begin{array}{c} \\ S \\ 1 \\ 2 \\ L \end{array} \begin{array}{c} \begin{array}{cccc} S & 1 & 2 & L \end{array} \\ \begin{bmatrix} 0 & 0.8102 & 0.0525 & -0.0047 \\ 0.8102 & 0 & 0.7195 & 0.0525 \\ 0.0525 & 0.7195 & 0 & 0.8102 \\ -0.0047 & 0.0525 & 0.8102 & 0 \end{bmatrix} \end{array}$$

$$M_2 = \begin{array}{c} \\ S \\ 1 \\ 2 \\ L \end{array} \begin{array}{c} \begin{array}{cccc} S & 1 & 2 & L \end{array} \\ \begin{bmatrix} 0 & 0.7903 & 0.0025 & -0.0101 \\ 0.7903 & 0 & 0.7 & 0.0025 \\ 0.0025 & 0.7 & 0 & 0.7903 \\ -0.0101 & 0.0025 & 0.7903 & 0 \end{bmatrix} \end{array}.$$

The coupling values in the matrixes are then transformed into practical values; for Filter-I, the external Q-factor $Q_E^{\mathrm{I}} = 101$ and the coupling coefficient $K_{12}^{\mathrm{I}} = 0.0108$; and for Filter-II, $Q_E^{\mathrm{II}} = 80$ and $K_{12}^{\mathrm{II}} = 0.014$ [23]. The extracted results of the proposed dual-band filter are shown in Fig. 4 [24]. Fig. 4(a) shows that Q_E^{I} and K_{12}^{I} are controlled by a_1 and d_1, respectively, and have no effect on Q_E^{II} and K_{12}^{II}, while Q_E^{II} and K_{12}^{II} are controlled by a_2 and d_2, respectively, and have no effect on Q_E^{I} and K_{12}^{I}, as shown in Fig. 4(b). In addition, we can simultaneously adjust the external Q-factors and coupling coefficients of these two bands, as shown in Fig. 4(c); the H_1 controls both K_{12}^{I} and K_{12}^{II}, while H_2 controls both Q_E^{I} and Q_E^{II}.

Then, by properly setting the suitable values specified in Fig. 4 to meet the calculated ones, the final desired performance is obtained, as shown in Fig. 5, with the combined responses of the coupling matrix (1) (CM-1) and the coupling matrix (2) (CM-2). The simulated results match very well

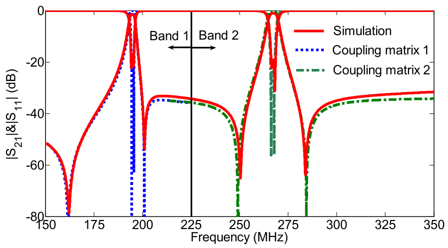

Fig. 5. Simulated and calculated *S*-parameters.

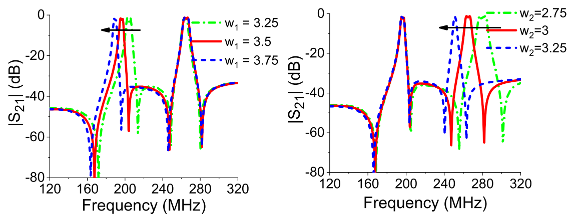

(a) (b)

Fig. 6. Individual frequency tuning. (a) First band. (b) Second band.

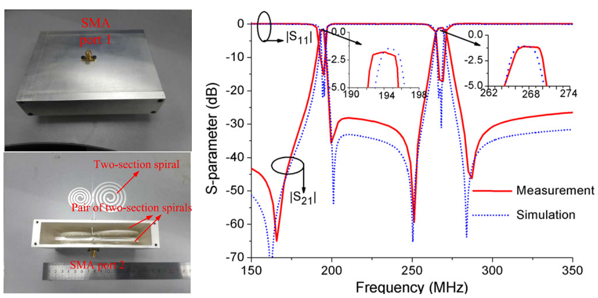

(a) (b)

Fig. 7. (a) Photograph. (b) Comparison of the simulated and measured results. The dimensions of the filter are (Unit: mm, except for n_1 and n_2): $a = 113$, $b = 84$, $c = 22.5$, $a_1 = 61$, $a_2 = 52$, $d_1 = 32.5$, $d_2 = 29.2$, $H = 8.8$, $p = 5.1$, $W = 1$, $r_1 = 2.5$, $g_1 = 2.75$, $w_1 = 3.5$, $h_1 = 2$, $n_1 = 4$, $r_2 = 2$, $g_2 = 1.5$, $w_2 = 3$, $h_2 = 2$, $n_2 = 4$.

with the combined responses of the two coupling matrixes. Each passband has two TZs in the out-of-band produced by the source–load coupling to obtain high selectivity. The first band works at 195 MHz with 1.6% FBW, 1.5-dB insertion loss (IL), and 17.2-dB RL, while the second band works at 267 MHz with 2% FBW, 1.1-dB IL, and 19.3-dB RL. The high IL of the filter is mainly due to the achievement of high selectivity and ultraminiaturized circuit size. In addition, the narrow bandwidth also contributes to the high IL.

Then, the individual frequency tuning of the two bands is provided. All the parameters r, g, w, and n can vary the total length to modify the resonant frequency. Here, we choose the sensitive parameters w_1 and w_2 for the analysis. Fig. 6(a) and (b) shows the frequency-tuning of the two bands: w_1 (for band 1) and w_2 (for band 2), respectively. The w_1 only influences the frequency of band 1, while w_2 only influences the frequency of band 2.

IV. Experimental Results and Discussion

To prove the design validity, the proposed second-order dual-band filter is fabricated and measured. The filter is fabricated using silver-plated brass based on the computer numerical control (CNC) technique with 0.01-mm machining accuracy. The photograph of the proposed filter is shown in Fig. 7(a). The comparison of the simulated and measured *S*-parameters is shown in Fig. 7(b), and a good agreement is achieved between them. From the measured results, we can see that the lower band works at 194 MHz with 1.7% FBW, 1.75-dB IL, and 13-dB RL, while the upper band works at 268 MHz with 2.1% FBW, 1.1-dB IL, and 16-dB RL. In addition, TZs on both sides of the two bands are achieved to produce high selectivity.

The comparison with other reported cavity dual-band filters is given in Table I, which indicates that the proposed filter has a miniaturized size, high selectivity produced by TZs on both sides of the passbands, and individual frequency tuning. The electrical sizes of the dual-band filters are calculated at the center frequencies of the lower band.

TABLE I

Comparisons With the Reported Cavity Dual-Band Filters

Ref.	Freq. (GHz)	Order	FBW	IL (dB)	Circuit Type	Size ($\lambda_0 \times \lambda_0 \times \lambda_0$)	TZs/Both sides	Individual Tuning
[14]	2.65/3.55	4	3-5%	0.34/0.39	Coaxial cavity	0.53×0.53×0.186	0/No	No
[15]	2.4/5.0	2	1%/1%	1.47/1.0	Capacitively-loaded cavity	0.51×0.41×0.2	2/No	Yes
[16]	4.25/4.55	3	1.5%/1.5%	1.3/1.15	Dielectric-loaded cavity	0.37×0.21×0.27	6/No	No
[18]	0.43/0.91	2	1.85%/0.77%	2.1/3.1	Helical cavity	0.055×0.032×0.042	0/No	No
This work	0.194/0.268	2	1.6%/2.1%	1.75/1.1	Spiral cavity	0.073×0.055×0.015	4/Yes	Yes

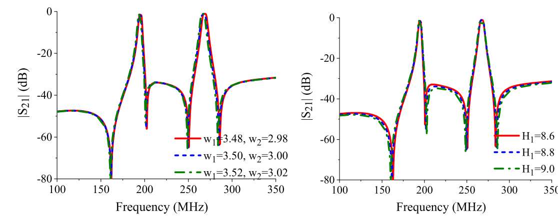

(a) (b)

Fig. 8. Sensitivity analysis. (a) Effect of w_1 and w_2. (b) Effect of the spacing H_1.

The fabrication tolerance and long-term effect of the proposed dual-band filter are subsequently discussed. The most sensitive parameters of fabrication tolerance are the width of turns and gaps between turns. Fig. 8(a) shows the performance tolerance with respect to the width of turns; the filtering performance almost remains unchanged for the variation of 0.04 mm (four times of the machining accuracy). For the consideration of the vibration in long-term usage, the spacing between the spirals is the main influenced dimension, i.e., H_1. The effect of H_1 is shown in Fig. 8(b), and it can be seen that for the variation of 0.4 mm, a small influence is produced.

V. Conclusion

A dual-mode resonator using two-section spirals with a reduced size is proposed to design the dual-band second-order bandpass filter. The working frequencies and filtering performances of the two bands can be individually designed. The proposed feeding structure naturally produces the source–load coupling to generate the two TZs on both sides of the passband to improve the passband's selectivity. In addition, the three supporting points can enhance the strength of the physical support. The measurement shows that the proposed dual-band filter has a miniaturized size and high selectivity.

REFERENCES

[1] S. Lee and Y. Lee, "A planar dual-band filter based on reduced-length parallel coupled lines," *IEEE Microw. Wireless Compon. Lett.*, vol. 20, no. 1, pp. 16–18, Jan. 2010.

[2] S. Zhang and L. Zhu, "Compact split-type dual-band bandpass filter based on $\lambda/4$ resonators," *IEEE Microw. Wireless Compon. Lett.*, vol. 23, no. 7, pp. 344–346, Jul. 2013.

[3] S. Zhang and L. Zhu, "Compact tri-band bandpass filter based on $\lambda/4$ resonators with U-folded coupled-line," *IEEE Microw. Wireless Compon. Lett.*, vol. 23, no. 5, pp. 258–260, May 2013.

[4] F.-C. Chen and Q.-X. Chu, "Design of compact tri-band bandpass filters using assembled resonators," *IEEE Trans. Microw. Theory Techn.*, vol. 57, no. 1, pp. 165–171, Jan. 2009.

[5] X. Yin Zhang and Q. Xue, "Novel dual-mode dual-band filters using coplanar-waveguide-fed ring resonators," *IEEE Trans. Microw. Theory Techn.*, vol. 55, no. 10, pp. 2183–2190, Oct. 2007.

[6] H. Zhang, W. Kang, and W. Wu, "Miniaturized dual-band SIW filters using E-shaped slotlines with controllable center frequencies," *IEEE Microw. Wireless Compon. Lett.*, vol. 28, no. 4, pp. 311–313, Apr. 2018.

[7] S. Amari and M. Bekheit, "A new class of dual-mode dual-band waveguide filters," *IEEE Trans. Microw. Theory Techn.*, vol. 56, no. 8, pp. 1938–1944, Aug. 2008.

[8] L. Zhu, R. R. Mansour, and M. Yu, "Compact waveguide dual-band filters and diplexers," *IEEE Trans. Microw. Theory Techn.*, vol. 65, no. 5, pp. 1525–1533, May 2017.

[9] S.-W. Wong, Z.-C. Guo, J.-Y. Lin, L. Zhu, and Q. Zhang, "Triple-mode and triple-band cavity bandpass filter on triplet topology with controllable transmission zeros," *IEEE Access*, vol. 6, pp. 29452–29459, 2018.

[10] Z.-C. Guo, S.-W. Wong, and L. Zhu, "Triple-passband cavity filters with high selectivity under operation of triple modes," *IEEE Trans. Compon., Packag., Manuf. Technol.*, vol. 9, no. 7, pp. 1337–1344, Jul. 2019.

[11] F.-C. Chen, J.-M. Qiu, S.-W. Wong, and Q.-X. Chu, "Dual-band coaxial cavity bandpass filter with helical feeding structure and mixed coupling," *IEEE Microw. Wireless Compon. Lett.*, vol. 25, no. 1, pp. 31–33, Jan. 2015.

[12] S.-W. Wong *et al.*, "Individually frequency tunable dual- and triple-band filters in a single cavity," *IEEE Access*, vol. 5, pp. 11615–11625, Jul. 2017.

[13] S.-W. Wong, F. Deng, J.-Y. Lin, Y.-M. Wu, L. Zhu, and Q.-X. Chu, "An independently four-channel cavity diplexer with 1.1–2.8 GHz tunable range," *IEEE Microw. Wireless Compon. Lett.*, vol. 27, no. 8, pp. 709–711, Aug. 2017.

[14] E. Doumanis, L. Guan, G. Goussetis, and D. Ferling, "Dual-band bandpass double ground plane coaxial resonators and filters," *IEEE Trans. Microw. Theory Techn.*, vol. 66, no. 8, pp. 3828–3835, Aug. 2018.

[15] X. Liu, L. P. B. Katehi, and D. Peroulis, "Novel dual-band microwave filter using dual-capacitively-loaded cavity resonators," *IEEE Microw. Wireless Compon. Lett.*, vol. 20, no. 11, pp. 610–612, Nov. 2010.

[16] V. Nocella, L. Pelliccia, C. Tomassoni, and R. Sorrentino, "Miniaturized dual-band waveguide filter using TM dielectric-loaded dual-mode cavities," *IEEE Microw. Wireless Compon. Lett.*, vol. 26, no. 5, pp. 310–312, May 2016.

[17] E. Doumanis, G. Goussetis, and S. A. Kosmopoulos, "Inline interdigital pseudo-elliptic helical resonator filters," *IEEE Microw. Wireless Compon. Lett.*, vol. 21, no. 8, pp. 400–402, Aug. 2011.

[18] Q.-X. Chu and Z.-C. Zhang, "Dual-band helical filters based on nonuniform pitch helical resonators," *IEEE Trans. Microw. Theory Techn.*, vol. 65, no. 8, pp. 2886–2892, Aug. 2017.

[19] R.-S. Chen, S.-W. Wong, J.-Y. Lin, and Y. He, "Miniaturized microwave filter using circular spiral resonators in a single metal cavity," in *IEEE MTT-S Int. Microw. Symp. Dig.*, Jun. 2019, pp. 1347–1350.

[20] C.-K. Liao and C.-Y. Chang, "Design of microstrip quadruplet filters with source-load coupling," *IEEE Trans. Microw. Theory Techn.*, vol. 53, no. 7, pp. 2302–2308, Jul. 2005.

[21] R. J. Cameron, "General coupling matrix synthesis methods for Chebyshev filtering functions," *IEEE Trans. Microw. Theory Techn.*, vol. 47, no. 4, pp. 433–442, Apr. 1999.

[22] R. J. Cameron, "Advanced coupling matrix synthesis techniques for microwave filters," *IEEE Trans. Microw. Theory Techn.*, vol. 51, no. 1, pp. 1–10, Jan. 2003.

[23] R. J. Cameron, C. M. Kudsia, and R. R. Mansour, *Microwave Filters for Communication Systems: Fundamentals, Design, and Applications*. New York, NY, USA: Wiley, 2007.

[24] J.-S. Hong and M. J. Lancaster, *Microstrip Filters for RF/Microwave Applications*. New York: Wiley, 2001.